Volume 238, number 1, 43–48 FEB 06318 September 1988

Location of divalent ion sites in acyl carrier protein using relaxation perturbed 2D NMR

Anne F. Frederick, Lewis E. Kay* and James H. Prestegard

Department of Chemistry, Yale University, New Haven, CT 06511 and **Laboratory of Chemical Physics, National Institute of Diabetes and Digestive and Kidney Diseases, National Institutes of Health, Bethesda, MD 20892, USA*

Received 22 July 1988

The T_1-accordion COSY experiment has been applied to acyl carrier protein (ACP) to locate the divalent ion binding sites in the protein using the paramagnetic ion, Mn^{2+}, as a substitute for Ca^{2+}. Replacement with Mn^{2+} leads to an enhancement of proton spin-lattice (T_1) relaxation rates. These enhancements have a $1/r^6$ distance dependence that makes them extremely useful in structural analyses. Ion-proton distances ranging from 3.0 to 9.0 Å have been obtained from this experiment and subsequently used as constraints in the molecular mechanics module of AMBER to refine a protein structure.

2D NMR; Mn^{2+}; Acyl carrier protein; Spin-lattice relaxation rate; AMBER

1. INTRODUCTION

Divalent cations, such as Mg^{2+} and Ca^{2+}, play essential roles in the function of many biological systems. Characterization of the sites that these ions occupy is, therefore, an important prerequisite to understanding biological function. A number of approaches to locating ion sites have been devised and applied to macromolecules in the past [1]. Here, we present a two-dimensional (2D) NMR approach to the structural characterization of an ion-binding site. The information obtained on ion site locations complements the more general structural descriptions now being accumulated on small soluble proteins using a 2D NMR approach [2,3].

The system with which we plan to illustrate our approach is a small protein, acyl carrier protein (ACP). Acyl ACPs function as preferred substrates for the fatty acid synthetase complex of most organisms by carrying fatty acids during the elongation process [4,5]. While ACP is not commonly regarded as a metalloprotein, Schulz et al. [6] observed a stimulation of fatty acid synthesis upon the addition of divalent cations that correlated with ion-induced changes in the structure of ACP. Two sites, each capable of binding Mg^{2+} or Ca^{2+}, have been proposed [7]. However, no detailed information on the location of these sites on ACP exists.

Recently, we completed a structural determination of *Escherichia coli* ACP using high-resolution NMR methods [8]. The determination was based on a nearly complete sequential assignment of resonances for protons along the backbone of the protein and on the use of cross-relaxation or nuclear Overhauser effects (NOEs) among these resonances to extract interproton distances [9]. Relaxation properties of the same resonances can

Correspondence address: J.H. Prestegard, Department of Chemistry, Yale University, New Haven, CT 06511, USA

Abbreviations: 2D, two-dimensional; ACP, acyl carrier protein; NOE, nuclear Overhauser effect; T_1, spin-lattice relaxation rate; T_2, spin-spin relaxation rate; COSY, coupling correlated spectroscopy; DTT, dithiothreitol; RMS, root mean square; AMBER, Assisted Model Building with Energy Refinement, a program licensed from the Regents of the University of California, Copyright 1986, UCSF

Published by Elsevier Science Publishers B.V. (Biomedical Division)
00145793/88/$3.50

also be useful in giving information about the location of the ion-binding sites. Spin relaxation properties of resonances from protons near the ion-binding sites can be selectively perturbed by the introduction of paramagnetic analogs of the normal ions [10]. The well known dependence of relaxation times on ion–proton distances ($1/r^6$), when the ion is a paramagnetic species, can be used to extract structural information in much the same manner as the $1/r^6$ dependence of cross-relaxation is used to extract proton–proton distances for the basic structure determination. The use of paramagnetic probes, however, offers some advantages in that the distances obtained span a longer range than those typically obtained from 2D NOE experiments [11].

Ion–proton distances can be determined from either spin-lattice (T_1) or spin-spin (T_2) relaxation time perturbations. Some experiments of this type have been pursued in the past, but T_2 perturbations are limited to rather qualitative interpretations [11], and existing 2D NMR methods used for T_1 determination are very time-consuming [12]. Recently, we introduced a pulse sequence based on the accordion experiment of Bodenhausen and Ernst [13,14] which enables extraction of T_1 values from a single 2D experiment. The pulse sequence for the T_1-accordion COSY (coupling correlated spectroscopy) experiment [15] is: $180_x - \varkappa t_1 - 90_{\phi_1} - t_1 - 90_{\phi_2} - t_2$ where $\varkappa$ is a factor chosen to sample effectively the longitudinal relaxation time course of the spins, and ϕ_1 and ϕ_2 represent rf phase shifts chosen to minimize spectral artifacts. The 2D spectrum shows the same cross-peaks as a normal phase-sensitive COSY spectrum, but T_1 recoveries are encoded in the line shapes in the ω_1 dimension.

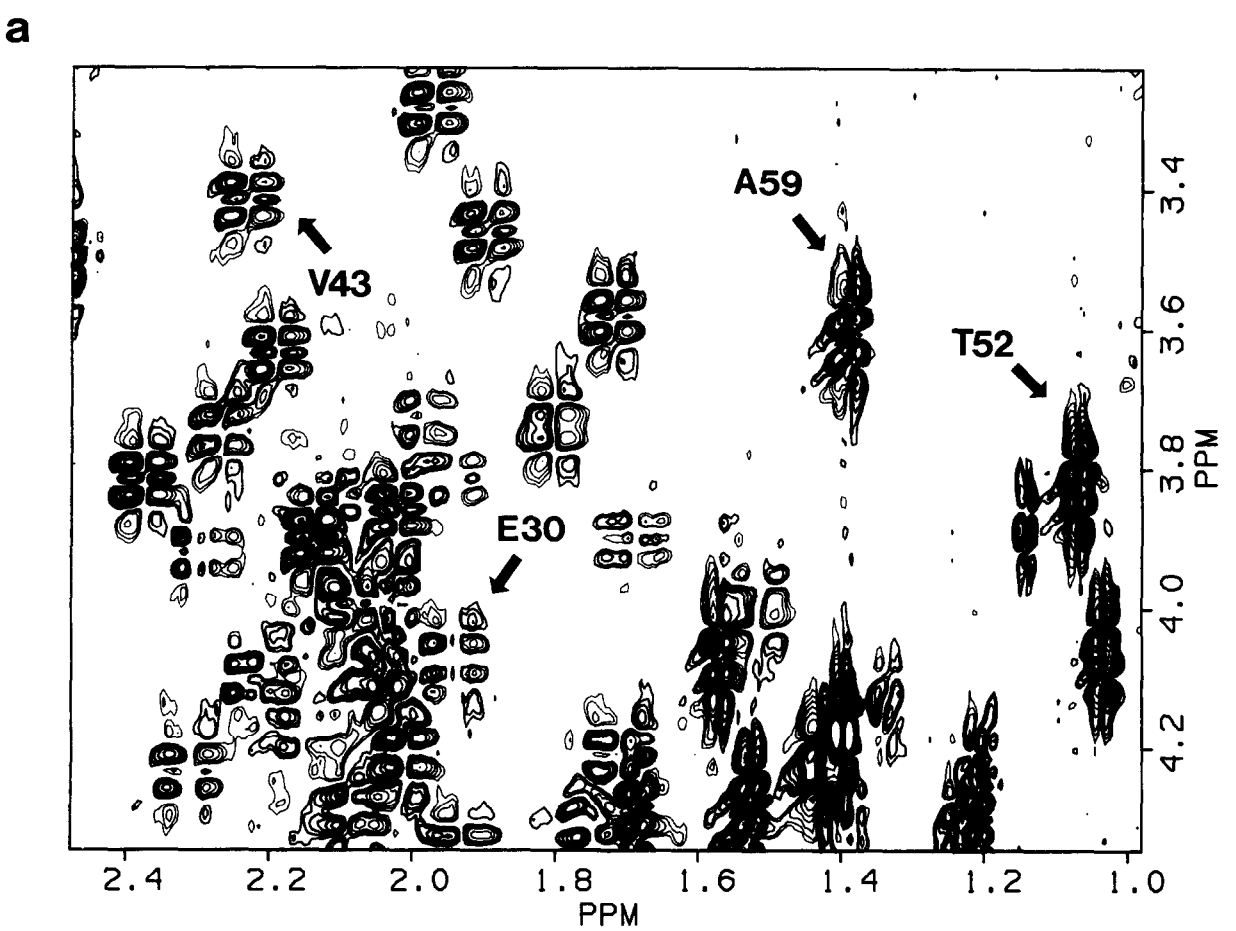

Fig.1. T_1-accordion COSY spectra of ACP without Mn^{2+} (a) and with Mn^{2+} (b). Note the loss in intensity in several of the cross-peaks in (b).

They can be extracted by appropriate processing procedures and interpreted in terms of distances.

Here, we will use this pulse sequence to investigate the ion-binding sites of ACP using the paramagnetic ion, Mn^{2+}, to substitute for Ca^{2+} or Mg^{2+}. Mn^{2+} shows moderately strong binding ($K_d = 10^{-4}$) for 1–2 sites depending upon the pH (unpublished) and upon the state of acylation (Mayo, K.H., personal communication). Exchange of Mn^{2+} into the sites on ACP is rapid on the NMR time scale, so fractional populations result in a small, uniform perturbation of all molecules in the sample. The degree of perturbation can be adjusted by adding Mn^{2+} in sufficiently small amounts to produce measurable perturbations without a complete loss of 2D cross-peaks. The ion–proton distances we obtain can then be used as constraints in molecular mechanics calculations in order to locate the ion-binding sites of the protein [9].

2. EXPERIMENTAL

ACP was isolated from *E. coli* B cells (Grain Processing) using the method of Rock and Cronan [16], and then reduced with dithiothreitol (DTT) to the free sulfhydryl form. Data were acquired on a 4 mM sample of ACP, 50 mM in KH_2PO_4, at pH 6.1 in D_2O. After the first data set was collected, a small aliquot of an $MnCl_2$ solution was added to the sample (~5 mol% with respect to ACP) and the second data set was collected.

NMR experiments were performed at 490 MHz on a home-built spectrometer. The data were generated from a double quantum filtered COSY accordion sequence [15] and recorded in the phase-sensitive mode using the method of States et al. [17]. The 2D spectra were collected as 400 t_1 experiments, each containing 2K complex data points over a spectral width of 5.0 kHz in both dimensions. For the first data set (ACP without Mn^{2+}), 80 scans were acquired per t_1 value with $x = 7.5$; the total time for this experiment was 74 h. For the second data set

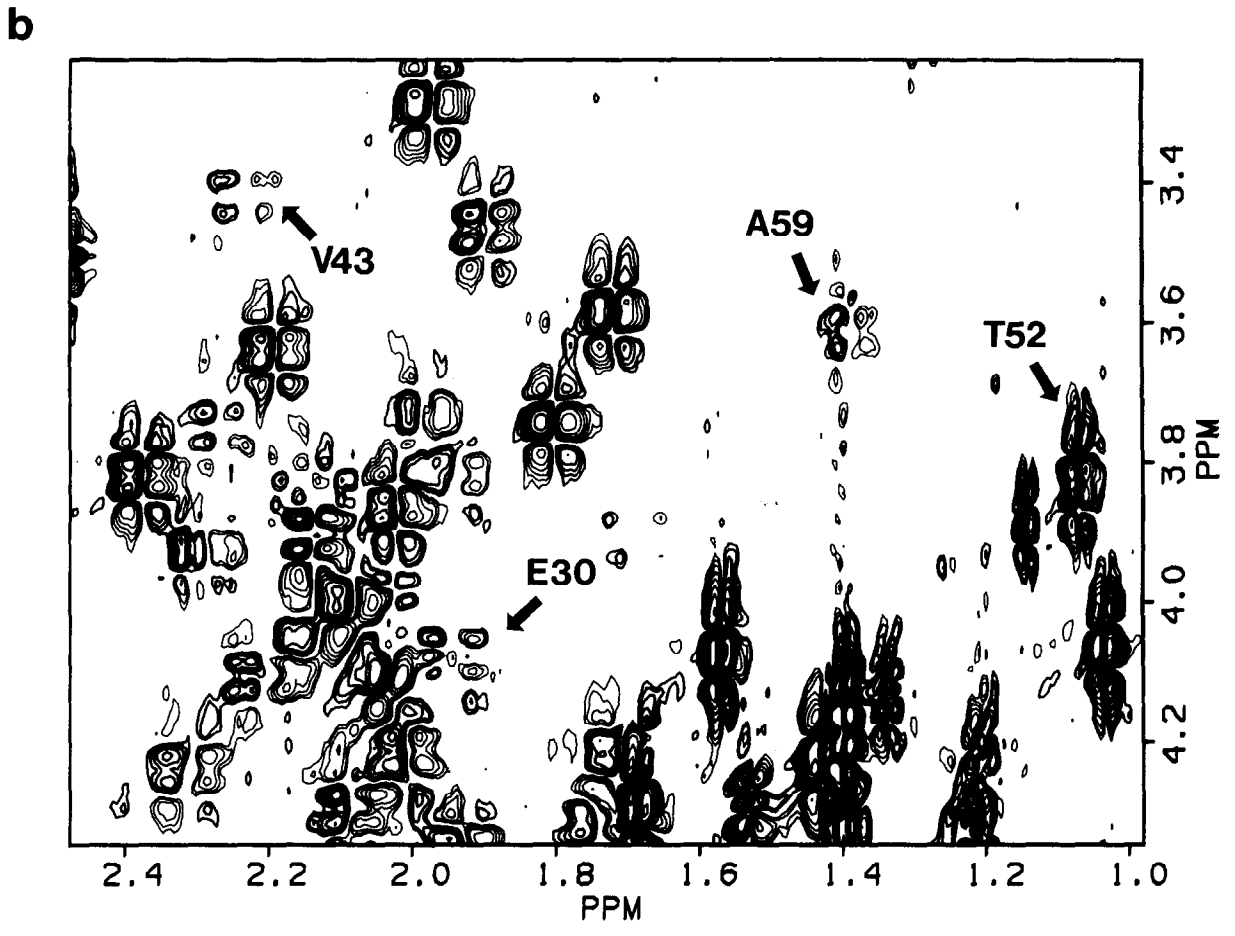

(ACP with Mn^{2+}), 88 scans were acquired per t_1 value with x = 5.0; the total time was 71 h. Recycle times of 2.0 s were used for both experiments. The data were processed on a Vax 11/750 computer equipped with a CSPI Minimap array processor. Data sets were multiplied in both dimensions by skewed sinebell squared functions (extending to 400 t_1 points) and zero-filled to 2K in the t_1 dimension before Fourier transformation.

Extraction of T_1 values was accomplished by loading a column of the frequency domain spectrum containing the cross-peak of interest and left or right shifting the data until a sufficiently narrow frequency band containing only the multiplet components associated with the desired cross-peak was obtained. The data were then inverse Fourier transformed and magnitude corrected to obtain the time course of the t_1 decay. Although a complete time course can be fit to inversion recovery curves [15], T_1 values were usually extracted from the first zero crossing and corrected to take into account the fact that, for the recycle times used in these experiments, magnetization recovers to a steady-state non-equilibrium value.

3. RESULTS AND DISCUSSION

Fig.1 shows T_1-accordion COSY spectra of ACP without Mn^{2+} (a) and with Mn^{2+} (b). Cross-peaks in the region plotted have been previously assigned [9] to αCH-βCH or βCH-γCH_3 cross-peaks for specific residues as indicated in fig.1. A loss in intensity in several of the cross-peaks (E30, V43, A59) is evident in the spectrum of ACP with Mn^{2+}. These changes in intensity would be observed even in a normal COSY spectrum because they are largely the result of extensive line broadening and are useful in giving qualitative information about which residues are nearest the ion-binding sites. However, other residues such as T52 are also perturbed without a substantial loss in intensity. We can demonstrate more quantitatively that the spin-lattice relaxation rates of residues such as T52 are enhanced by the presence of Mn^{2+} by examination of T_1 recovery curves for these particular residues.

Fig.2 shows the time course of the t_1 decay obtained by inverse Fourier transformation of the column containing the cross-peak for T52 ($\beta CH(\omega_1)$-$\gamma CH_3(\omega_2)$). The curve starts at zero because of the antiphase nature of the J-resolved cross-peaks. The null observed near xt_1 = 0.96 s is the zero crossing point in the T_1 inversion recovery curve for T52. It appears as a minimum rather than a zero crossing in fig.2 because a magnitude spectrum is displayed. T_1 values extracted from this curve correspond to longitudinal relaxation rates for the proton characterized by the frequency ω_1, in this case the βH of T52. The shift of the null

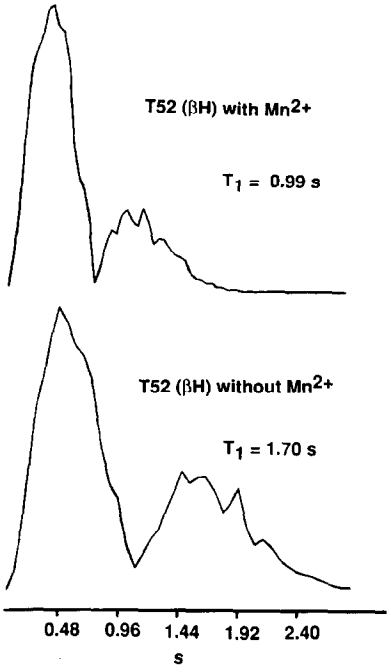

Fig.2. Null points of the βH of T52 with and without Mn^{2+}. The shift of the null upon the addition of Mn^{2+} makes it possible to obtain ion–proton distances even though the appearance of the cross-peak remains unchanged.

upon the addition of Mn^{2+} makes it possible to obtain quantitative information about changes in T_1 values (1.70 vs 0.99 s), even though the appearance of the cross-peak remains largely unchanged.

Mn^{2+} contributions to enhancements in T_1 relaxation rates can be quantitatively interpreted provided a suitable distance standard (r_0) can be obtained. It is highly probable that carboxyl groups of strongly perturbed glutamic acids are directly involved in the coordination of the ion. Assuming typical coordination geometry, the coordinated ion would be approx. 6 Å from the α-proton of such a glutamic acid residue.

The presence of two ion-binding sites on the protein necessitates choosing two calibration distances, and therefore assigning the perturbed residues to one site or the other. Fortunately, many of the resonances perturbed seem to cluster around two distinct, well-separated sites involving glutamic acids E30 and E48, respectively. Perturbations of these residues were used as standards for conversion of relaxation enhancement for other resonances to ion–proton distances (r) using

the known r_0^6/r^6 dependence. These sites are at opposite ends of a long α-helix in the structure [8] and thus resonances effected by Mn^{2+} can be assumed to be perturbed by only one ion site. Perturbed resonances were assigned to one site or the other using a program which searched all possible site assignments for the combination which allowed placement of the ions in the initial protein structure at sites which produced minimum RMS deviations from the observed distances. Some cross-peaks completely disappear upon the addition of Mn^{2+} preventing the measurement of T_1 values for such protons. A lower limit distance of 3 Å (or 4 Å in cases where there is only a pseudoatom present in the molecular mechanics program) has been assigned for these cross-peaks. All the resulting experimental ion–proton distances constraints are summarized in table 1. Note that there are several long-range distance constraints extending out to 8.8 Å. In addition to locating ion sites, these long-range constraints are extremely useful in refining the structure of the protein obtained from 2D NOE experiments.

The molecular mechanics module of AMBER [18,19] was used to obtain refined structures in the presence of ion-proton constraints. Structures previously minimized by our laboratory using NOE distance constraints alone were used as starting structures [8]. Counterions (two Ca^{2+}) were initially placed at the sites described above and force field parameters, that had been optimized to reproduce the structure of calcium di-L-glutamate [20], were used to represent ion properties. Ion–proton distance constraints were then applied as pseudoenergies along with existing NOE distance constraints. The structure was minimized following a protocol described previously that entails an initial convergence with high pseudoenergy weights, in the presence of bond and bond angle constraints, followed by a convergence at low weights with all energy terms present [8]. This process required 14 h on a Multiflow Trace-7 computer, and was repeated using 2 different starting structures. One of the starting structures, with initial ion placements and dashed lines denoting constraints, is shown in fig.3a; the final structure is shown in fig.3b. Site A appears to utilize E30, D35 and D38 in its ion coordination. Site B is near a proline-containing bend and appears to involve stronger interactions with E47, D51, E53 and D56 than with the calibration residue, E48. This suggests caution should be exercised in the quantitative interpretation of site B.

Table 1

Ion-proton distances for the ACP-Mn^{2+} complex

Ion	Proton[a]	Distance (Å)
A	L15 HG	3.00[b]
	L15 CB	4.00[b]
	A34 HB	3.00[b]
	D35 CB	4.00[b]
	D38 CB	4.00[b]
	E30 HA	6.00
	V40 HA	6.28
	K18 HA	6.90
	I11 HA	6.97
	F28 CG	8.54
	F28 CB	8.81
B	I54 HB	3.00[b]
	I54 CG	4.00[b]
	M44 CB	4.00[b]
	E47 CB	4.00[b]
	D51 CB	4.00[b]
	E53 CB	4.00[b]
	P55 CB	4.00[b]
	D56 CB	4.00[b]
	A45 HA	5.19
	E48 HA	6.00
	V43 HA	6.07
	T52 HB	6.39
	A59 HA	6.73

[a] Proton designations use one-letter codes for amino acid types followed by residue number and atom names as employed in AMBER

[b] Estimated distances based on disappearance of cross-peaks

RMS deviations for ion-proton constraints improve from 2.7 to 1.5 for site A and from 3.6 to 1.1 for site B during convergence. Surprisingly, the RMS deviation of NOE constraints obtained for the protein backbone atoms in the absence of ions is unchanged by the minimization process (0.9 Å). The protein structure does change during minimization as can be seen in fig.3 and in the RMS deviation of backbone atomic positions in the final structure relative to the initial structure of 2.9 Å. This suggests that the structural changes have occurred in parts of the structure that were poorly defined by NOE constraints.

The T_1-accordion COSY experiment described above thus provides an excellent method for locating the ion-binding sites of a protein through

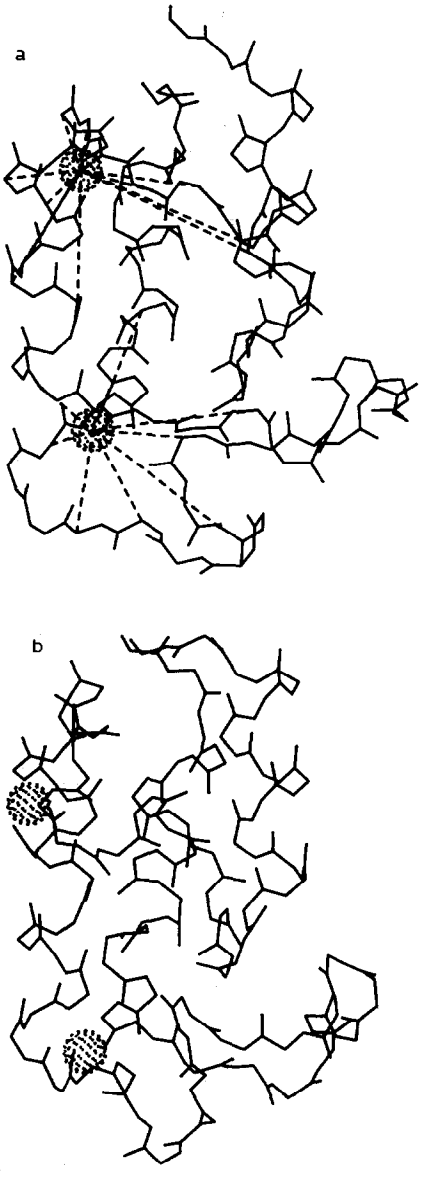

Fig.3. Starting structure of ACP with initial ion placements and dashed lines representing constraints (a) and the final minimized structure of ACP with ions (b).

the use of a paramagnetic probe such as Mn^{2+}. Also, the relatively long ion–proton distances that are obtained from this experiment give conformational information that can be used in structure refinement and can complement distances obtained by more conventional 2D NOE experiments.

Acknowledgements: This work was supported by Grant GM-32243 from the National Institutes of Health and benefitted from instrumentation acquired under NIH Grant RR03822. A.F.F. acknowledges predoctoral support from the Heyl Foundation. L.E.K. acknowledges a predoctoral fellowship from the Natural Sciences and Engineering Research Council of Canada.

REFERENCES

[1] Forsén, S., Drakenberg, T. and Wennerström, H. (1987) Q. Rev. Biophys. 19, 83–114.
[2] Havel, T.F. and Wüthrich, K. (1985) J. Mol. Biol. 182, 281–294.
[3] Williamson, M.P., Havel, T.F. and Wüthrich, K. (1985) J. Mol. Biol. 182, 295–315.
[4] Thompson, G.A. jr (1981) in: The Regulation of Membrane Lipid Metabolism, pp.19–23, CRC, Boca Raton, FL.
[5] Wakil, S.J., Stoops, J.K. and Joshi, V.C. (1983) Annu. Rev. Biochem. 52, 537–579.
[6] Schulz, H., Weeks, G., Toomey, R.E., Shapiro, M. and Wakil, S.J. (1969) J. Biol. Chem. 244, 6577–6583.
[7] Schulz, H. (1972) Biochem. Biophys. Res. Commun. 46, 1446–1453.
[8] Holak, T.A., Kearsley, S.K., Kim, Y. and Prestegard, J.H. (1988) Biochemistry, in press.
[9] Holak, T.A. and Prestegard, J.H. (1986) Biochemistry 25, 5766–5774.
[10] Gariepy, J., Kay, L.E., Kuntz, I.D., Sykes, B.D. and Hodges, R.S. (1985) Biochemistry 24, 544–550.
[11] Schmidt, P.G. and Kuntz, I.D. (1984) Biochemistry 23, 4261–4266.
[12] Arseniev, A.S., Sobol, A.G. and Bystrov, V.F. (1986) J. Magn. Reson. 70, 427–435.
[13] Bodenhausen, G. and Ernst, R.R. (1981) J. Magn. Reson. 45, 367–373.
[14] Bodenhausen, G. and Ernst, R.R. (1982) J. Am. Chem. Soc. 104, 1304–1309.
[15] Kay, L.E. and Prestegard, J.H. (1988) J. Magn. Reson. 77, 599–605.
[16] Rock, C.O. and Cronan, J.E. jr (1981) Methods Enzymol. 71, 341–351.
[17] States, D.J., Haberkorn, R.A. and Ruben, D.J. (1982) J. Magn. Reson. 48, 286–292.
[18] Weiner, S.J., Kollman, P.A., Case, D.A., Singh, U.C., Ghio, C., Alagona, G., Profeta, S. jr and Weiner, P.K. (1984) J. Am. Chem. Soc. 106, 765–784.
[19] Weiner, S.J., Kollman, P.A., Nguyen, D.T. and Case, D.A. (1980) J. Comput. Chem. 7, 230–252.
[20] Einspahr, H. and Bugg, C.E. (1979) Acta Crystallogr. B35, 316–321.